

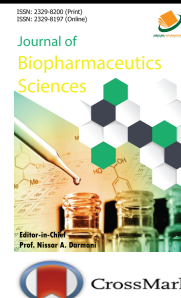


ISSN: 2329-8200 (Print)
ISSN: 2329-8197 (Online)

CODEN : JBSOC4

Journal of Biopharmaceutics Sciences (JBS)

DOI : <http://doi.org/10.26480/jbs.02.2017.10.14>



PREPARATION AND CHARACTERIZATION OF PUERARIN NANOSUSPENSION BY ANTI-SOLVENT PRECIPITATION

Chongkai Gao^{1*}, Bohong Guo¹, Danqiao Xu¹, Jin Li¹, Yihua Chen¹, Xiaofang Li¹, Chenchen Jin¹, Keqing Zhang²

¹School of pharmacy, Guangdong Pharmaceutical University, Guangzhou 510000, China

²Henan Vocational College of Chemical Technology, Zhengzhou 450000, China

*Corresponding Author's E-mail: godck01@163.com

This is an open access article distributed under the Creative Commons Attribution License, which permits unrestricted use, distribution, and reproduction in any medium, provided the original work is properly cited

ARTICLE DETAILS

Article History:

Received 12 July 2017
Accepted 10 August 2017
Available online 15 September 2017

ABSTRACT

The aim of this study was to prepare and characterize puerarin nanosuspension to enhance the dissolution rate and oral bioavailability of this drug. Nanosuspension was prepared by the anti-solvent precipitation method. The particle size and zeta potential of nanosuspension were 195 nm (\pm 8 nm) and -12.5 mV (\pm 1.2 mV), respectively. The morphology of nanosuspension was found to be flaky-shaped by scanning electron microscopy (SEM) observation. The X-ray powder diffraction (XRPD) and differential scanning calorimetry (DSC) analysis confirmed that the nanosuspension was in the amorphous state. The flow-through cell was considered to be the most robust dissolution method for the nanoparticulate system. The dissolution rate of nanosuspension was significantly increased by reducing the particle size. The dissolution testing in water showed that the nanosuspension exhibited significantly a higher dissolution rate with 71.9% drug dissolved in 5 min as compared to the raw puerarin (15.2%).

KEYWORDS

Puerarin, nanosuspension, anti-solvent precipitation, dissolution.

1. INTRODUCTION

Based on a study, Nanosuspension refers to nanoparticles, which were composed of 100% drug without any matrix material and with a mean particle size below 1 μ m [1]. As a matter of fact, they are a kind of the stabilizing system formed from a dispersion of nanosized drug particles using a suitable stabilizer. Nanosuspension can enlarge surface area, enhance saturation solubility, and increase dissolution rate, which result in an increased and consistent oral bioavailability. Nanosuspension technology becomes a universal formulation approach to processing drugs with low solubility. Study showed an important advantage of nanosuspension is that they can be applied to various administration routes: oral, parenteral, ocular, pulmonary, dermal [2-6].

The preparation methods of nanosuspension can be grouped into two principal classes: "bottom-up" and "top-down" technologies. The "top-down" technology includes various wet milling methods such as using high pressure homogenizers and using the mill medium to produce nanosuspension [7]. Although "top-down" technologies are widely employed, the drawbacks associated with mechanical attritions processes, such as time and energy consumption, inadequate control of particles size and morphology, promote greater interest toward "bottom-up" creation of nanosuspension [8]. The "bottom-up" technology starts at the molecular level and proceeds to the formation of a solid nanosized particle, including the anti-solvent precipitation technique, supercritical anti-solvent (SAS), rapid expansion of supercritical solution (RESS), spray-freezing into liquid process, evaporative precipitation into aqueous solution (EPAS) and liquid anti solvent (high-gravity controlled precipitation and sono precipitation) [9]. Among them, anti-solvent precipitation was reported as a simple and cost effective promising alternative with scale-up potential [10]. For a typical anti-solvent precipitation, an organic drug solution is introduced to the anti-solvent under rapid mixing, which generates high

supersaturation and thereby the fast nucleation rate leading to production of particles in the nanometer (1-1000 nm) range.

Puerarin (8-beta-D-glucose pyranose 4'-7-dihydroxyisoflavone) is one of the main effective elements of isoflavones, a constituent in Leguminous Pueraria. It plays role on blood vessel dilatation, lowering blood pressure and myocardial oxygen consumption, and improving coronary artery blood flow and microcirculation [11-13]. However, the poorly soluble puerarin has suffered from low bioavailability. So that intravenous injection is adopted clinically. According to a researcher, intravenous injection of puerarin has severe acute side effects such as hemolysis [14]. In order to increase the drug solubility and bioavailability, pure drug nanoparticle delivery systems can be better choices.

The purpose of this work is to produce puerarin nanosuspension for dissolution rate enhancement. For the drug of puerarin, nanosuspension have been produced by high pressure homogenization [15]. In this work, we prepared puerarin nanosuspension by anti-solvent precipitation technique, which has not been reported in the literature, to our knowledge. In this process, water was used as the anti-solvent for the precipitation of puerarin. The appropriate solvent and stabilizer were screened by investigating the size of the precipitated particles. Dynamic laser light scattering technique (DLS) was used to measure the particle size. Effects of surfactant type on particle size were investigated. Morphology and thermal behavior of the raw puerarin and nanosuspension were examined by SEM and DSC, respectively. Also, FTIR was used to investigate the drug chemical structure. Saturation solubility was tested by high performance liquid chromatography (HPLC). Finally, dissolution profiles of raw puerarin and nanosuspension were studied by USP Apparatus IV (Flow-through cell) method.

2. MATERIAL AND METHODS

2.1 Material

Puerarin (purity $\geq 99\%$) was purchased from Shanghai DND Pharm-Technology Co., Inc. (Shanghai, China). Sodium dodecyl sulfate (SDS) and HPMC (E15) were kindly gifted by Anhui Sunhere Pharmaceutical Excipients Co., Ltd. (Anhui, China). Polyvinyl alcohol (PVA) was from Aldrich Chemistry (Germany). Polyvinylpyrrolidone (PVP) K30 and Lutrol F68 (poloxamer 188, a polyoxyethylene-polyoxyethylene triblock copolymer) were kindly gifted by BASF (D-Ludwigshafen, Germany). Tween 80 (polysorbate 80) was purchased from Yuxiang Chemical Reagent Co., Ltd. (Guangzhou, China). Methanol and acetonitrile (HPLC grade reagent) were obtained from Merck Inc. (Darmstadt, Germany). All the other reagents used were of analytical grade. Double distilled water was used throughout the experiments.

2.2 Preparation of Puerarin Nanosuspension

Based on a study, Puerarin nanosuspension was prepared through the anti-solvent precipitation method [16]. Briefly, puerarin was dissolved completely in methanol to prepare for organic phase and the solution was then passed through a 0.45 μm Millipore syringe filter to remove the possible impurities. Meanwhile, the anti-solvent phase was prepared by dispersing stabilizer PVP K30 in distilled water (0.1%). At a fixed temperature, 1 mL of organic solution (60 mg/mL) was quickly injected by syringe into 10 mL of anti-solvent using a magnetic stirring apparatus and continues stirring 10 min. The drug particles precipitated immediately from the anti-solvent. Then, the nanosuspension was kept under vacuum at room temperature to remove the methanol.

For long-term stability of the final product, the freshly prepared nanosuspension was spray dried using a Lab Spray Dryer L-117 from Laiheng Lab-Equipments Corporation (Beijing, China). Spray drying was conducted at inlet temperatures 150°C. Outlet temperature was 90

2.3 HPLC Conditions

The chromatographic system consisted of an HPLC System (Shimadzu LC-10 Avp, Japan) and a UV detector. The HPLC separation was performed on reverse phase C18 columns (5 μm , 4.6 \times 250 mm, Kromasil, Sweden). The mobile phase consisted of a mixture of methanol and 0.1% citric acid (25:75, v/v). The mobile phase was filtered through a 0.45 μm microporous membrane and was deaerated ultrasonically prior to use. The detector was set at 250 nm and the flow rate were set at 1 mL/min. The column temperature was set at 30°C.

2.4 Vesicle Size and Zeta-potential Analysis

Dry powders were reconstituted in water and the particle size was measured. The determination of the particle size and the polydispersity index (P.I.) of the nanosuspension were performed by DLS, using a Delsa Nano S Particle Analyzer (Beckman coulter Instruments, Fullerton, CA, USA). Zeta potential was measured by Nano Particle Analyzer (Beckman coulter Instruments, Fullerton, CA, USA). All measures were determined in triplicate at room temperature.

2.5 Scanning Electron Microscopy

Puerarin, PVP K30, physical mixture and nanosuspension were examined by SEM to visualize the surface morphology. Samples were prepared by making the film on aluminum to a thickness of 200-500 Å under an argon atmosphere using a gold sputter module in a high vacuum evaporator. The coated samples were scanned, and photographs were taken with SEM (LEO 1430 VP, Germany).

2.6 Powder X-ray Diffractometry

Crystal structure of puerarin, PVP K30, physical mixture and nanosuspension was studied using a powder X-ray diffractometer (XRD, D/max-III A, Cu K α , λ = 1.5406 Å, Rigaku Corporation, Japan) using Ni

filtered, a voltage of 35 kV and a current of 25 mA. The scanning rate employed was 1 /min over the 5-35 diffraction angle (2 θ) range.

2.7 Differential Scanning Calorimetry

The characteristic thermal peaks of puerarin, PVP K30, physical mixture and nanosuspension were examined using differential scanning calorimetry (DSC, Perkin Elmer DSC 4000, San Jose, California, United States Waltham, USA) thermal analyzer. Nitrogen was used as a carrier gas. DSC analysis was carried out at a heating rate of 10°C/min with a nitrogen flow rate of 300 mL/h. The sample amounts were 5 mg and endothermic peak was recorded at a temperature range between 30-280°C.

2.8 Fourier-transform Infrared Spectroscopy

FTIR was recorded for puerarin, PVP K30, physical mixture and nanosuspension using Spectrum 100 (Perkin Elmer, San Jose, California, United States) infrared spectrophotometer. Samples were prepared in KBr disc (2 mg sample /200 mg KBr) with a hydrostatic pressure at a force of 40 psi for 4 min. The scanning range used was 450-4000 cm^{-1} .

2.9 Saturation Solubility Studies

The saturation solubilities of both species were determined by adding an excess of each species (i.e. 50 mg and 100 mg for the raw puerarin and nanosuspension, respectively) in 20 mL of distilled water in stoppered conical flasks. The samples were initially sonicated for 15 min to fully disperse the powders into the fluid. The conical flasks were placed in a shaking water bath for 48 h to ensure that the solubility equilibrium had been reached. Subsequently, the saturated solutions were immediately centrifuged, and supernatant solution was filtered through 0.45 μm Millipore syringe filter and properly diluted with distilled water to prevent crystallization. Each experiment was performed in triplicate and the filtered and diluted solutions were analyzed by HPLC method.

2.10 Dissolution Studies

USP Apparatus I (Basket): Dissolution studies were performed in triplicate in a dissolution test apparatus (ZRS-8 G dissolution test apparatus, Tianjin, China) using the basket method (USP Apparatus I). A precisely weighted amount of powder equivalent to 100 mg puerarin was placed into the baskets and introduced into three vessels of the dissolution tester. The dissolution medium employed was 250 mL of distilled water. Basket speed and bath temperature were maintained at 100 rpm and 37.0 \pm 0.5°C, respectively. The samples (5 mL) were withdrawn with an equal volume of fresh distilled water supplemented at 2, 5, 10, 20, 30, 40, 50 and 60 min, filtered through a 0.45 μm Millipore syringe filter and analyzed in a UV-Visible spectrophotometer (Perkin Elmer, San Jose, California, United States) at 250 nm. Sink conditions were maintained throughout the dissolution testing period.

USP apparatus II (Paddle): The procedure was the same as the above except that the 100 mg samples were introduced directly into the vessels without the basket.

USP apparatus IV (Flow-through cell): 250 mL dissolution medium at 37.0 \pm 0.5°C was passed through a flow-through cell (SOTAX CE7, Switzerland) containing 100 mg of sample and re-circulated in a closed-loop configuration [17]. The flow rate of the dissolution medium through the cells was 16 mL/min. At regular time intervals, 5 mL samples were withdrawn, and their concentrations were analyzed in a UV-Vis spectrophotometer at 250 nm. Studies were carried out in triplicate.

3. RESULTS AND DISCUSSION

3.1 Particle Size, Zeta potential and Morphology

The particle size and zeta potential of nanosuspension were shown in Table 1. The mean particle size of nanosuspension was 195 nm with a polydispersity index of 0.193. The zeta potential was -12.5 mV. According to a study, it is usually recognized that the PI values between 0.10 and 0.20

Table 1: Mean particle size and zeta potential of puerarin nanosuspensions (means \pm S.D. n=6).

Mean particle size (nm)	Size distribution (nm)			Zeta potential (mV)	Polydispersity Index
	D10	D50	D90		
195 \pm 8	65 \pm 2	168 \pm 21	288 \pm 11	-12.5 \pm 1.2	0.193 \pm 0.05

are narrow distributions and the values between 0.25 and 0.50 are brand distributions [18].

Figure 1 presents the morphologies of raw puerarin, PVP K30, physical mixture and nanosuspension. Figure 1A shows that the puerarin has irregular shapes with particle size generally larger than 20 μm . As shown in Figure 1 D, the nanosuspension generated by precipitation was flaky in shape and diameters slightly less than 200 nm. The nanoparticle size observed by SEM was in good agreement with that determined by DLS, which was almost below 200 nm.

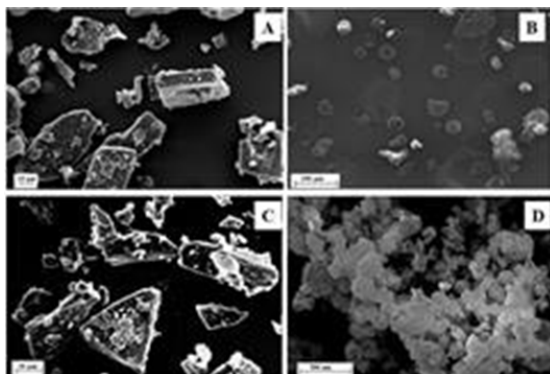


Figure 1: SEM micrographs of (A) puerarin, (B) PVPK₃₀, (C) physical mixture and (D) nanosuspension, Magnifications: A at 500 \times , B at 100 \times , C at 500 \times and D at 2000 \times .

To effectively prevent the aggregation between particles macromolecules and surfactants are added to the aqueous phase. The polymers most frequently used are polypropylene oxide polyethylene oxide block copolymers (Pluronic® or Poloxamers®), PVA or PVP. Surfactants are one of the most important factors of enabling the puerarin nanosuspension to be stable, which should offer sufficient affinity for the droplet surface to stabilize the nanosuspension. The molecular weights of these polymers are usually between 50 kDa and 100 kDa, and their chains should be long enough to provide a steric layer but not too large to slow down dissolution. The polymer has a good surface affinity and could form a substantial mechanical and thermodynamic barrier at the interface. In preliminary experiments, we selected the surfactants and polymers that were most frequently used, such as Poloxamer 188, PVP K30, Tween 80, SDS, HPMC, and PVA. The size, PI, and zeta potential of nanosuspension were determined as evaluation index. On the basis of the results, the PVP K30 was optimized as stabilizer.

3.2 X-ray Analysis

X-ray diffraction has been used to analyze potential changes in the inner structure of raw puerarin and nanosuspension (Figure 2). The raw puerarin displayed numerous distinct peaks at 2 θ of 6.42, 7.90, 11.54, 14.45, 15.87, 16.7, 18.83, 19.54, 21.02, and 23.28, while the nanosuspension displayed a smooth line with no characteristic peaks. This evidence supports the view that the crystalline structure had been lost as a result of the process of precipitation and drying.

3.3 DSC analysis

In order to further confirm the physical state, DSC was also performed to analyze the different samples. The crystalline structure was assessed by comparing the DSC thermal of raw puerarin and nanosuspension. The raw puerarin had a sharp melting endothermic peak at 219 $^{\circ}\text{C}$ ($\Delta H = 45.79$ J/g)

(Figure 3A). Being amorphous and very hygroscopic, PVP did not show any fusion peak or phase transition, apart from a broad endotherm due to dehydration between 80 and 120 $^{\circ}\text{C}$ (Figure 3B).

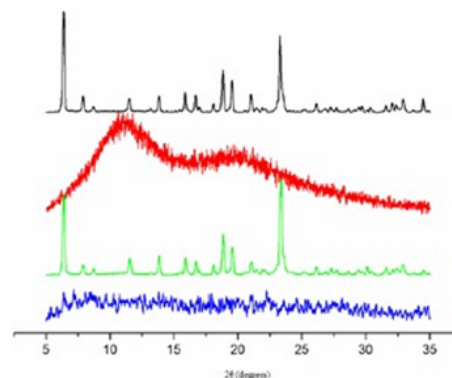


Figure 2: XRD of (A) puerarin, (B) PVPK₃₀, (C) physical mixture and (D) nanosuspension.

In the thermal curve of the physical mixture, the fusion endothermic peak of puerarin was slightly lower than that of the crystalline substance ($\Delta H = 31.55$ J/g) (Figure 3C). In contrast, this peak disappeared completely in the DSC thermal profile of nanosuspension (Figure 3D), suggesting an amorphous state of these particles. Based on a research, since the heat of fusion is proportional to the amount of crystallinity in the samples, these results suggested that the crystallinity of puerarin particles decreased when they were prepared into nanosuspension, which was also supported by the X-ray analysis results [19].

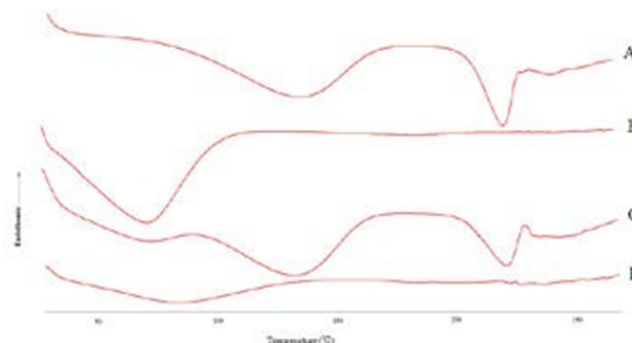


Figure 3: DSC of (A) puerarin, (B) PVPK₃₀, (C) physical mixture and (D) nanosuspension.

3.4 FTIR Analysis

The FTIR spectrum of puerarin is characterized by conjugated C=O stretching, 1634.60 cm^{-1} ; C-O, 1178.49 and 1060.08 cm^{-1} ; C=C, 1607.2, 1568.51, 1515.65 and 1448.05 cm^{-1} ; O-H, 3360.34 and 3233.18 cm^{-1} ; CH₂, 2901.52 cm^{-1} ; and C-C (benzene), 893.9, 836.7 and 798 cm^{-1} (Figure 4A). The FTIR spectrum of pure PVP K30 is characterized by O-H stretching, 3383.40 cm^{-1} and C=O, 1657.63 cm^{-1} (Figure 4B). An overlapped spectrum pattern was observed for the physical mixture (Figure 4C). Compared with physical mixture, the characteristic peaks of nanosuspension were different (Figure 4D). The O-H absorption bands of puerarin shifted to lower frequencies from 3360.34 and 3233.18 to 3129.90 cm^{-1} . The shape of the stretching band is broader and less intense in the spectrum of the nanosuspension than that of the physical mixture. In the spectrum of the nanosuspension, C=O stretching, C=C alkene stretching and C=C aromatic stretching shifted or weakened. This may be explained on the basis of hydrogen bonding between the drug molecules and the polymer [20-21].

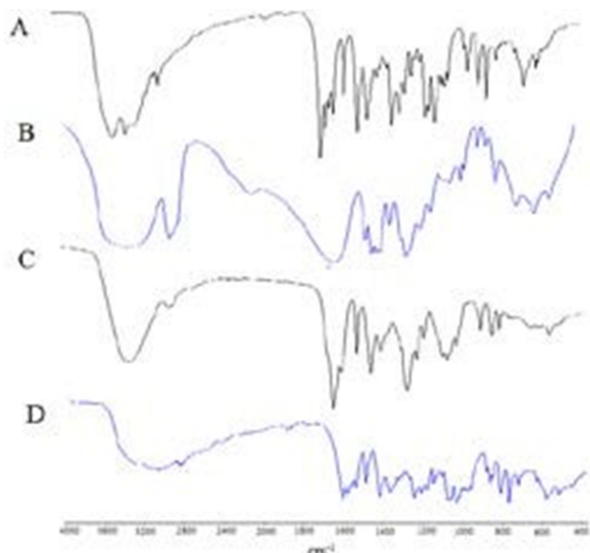


Figure 4: FTIR spectra of (A) puerarin, (B) PVPK30, (C) physical mixture and (D) nanosuspension.

3.5 Saturation Solubility

Although saturation solubility is defined as a compound-specific, temperature-dependent constant, it also depends on particle size. When the particle size is reduced to the nanometer range, the solubility of drugs will increase significantly. The increase in solubility can be explained by the Ostwald-Freundlich equation (1). According to Equation (1), the increased saturation solubility is due to creation of high-energy surfaces when the more or less ideal drug microcrystals are disrupted to nanoparticle [22].

$$\log \frac{C_s}{C_\infty} = \frac{2\nu\sigma}{2.303RT\rho r} \quad 1$$

Where C_s is the solubility, C_∞ is the solubility of the solid consisting of large particles, σ is the interfacial tension, ν is the molar volume of the particle material, R is the gas constant, T is absolute temperature, ρ is the density of the solid, and r is the radius of particles material. As illustrated in Figure 5, it was found that the saturation solubility was improved as the particle size of puerarin reduced. The saturation solubility in aqueous was 2.78 mg/mL and 5.28 mg/mL for raw puerarin and nanosuspension, respectively.

Therefore, formulating the poorly water-soluble puerarin as nanosuspension had a dramatic effect on the drug solubility.

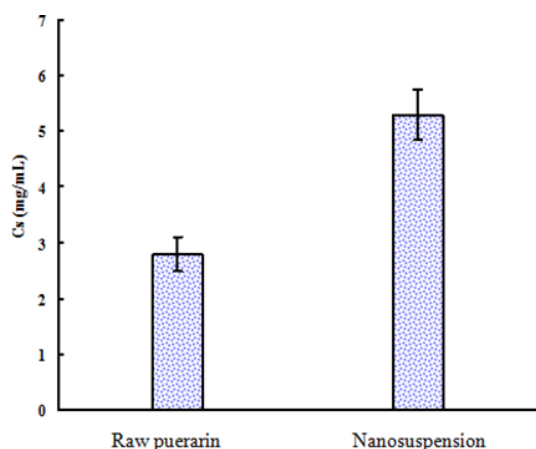


Figure 5: Saturation solubility of raw puerarin and nanosuspension.

3.6 In vitro dissolution test

Particle size reduction leads to enhancement in dissolution rates in accordance with the Noyes-Whitney equation (2): Particle-size reduction of drug particles leads to an increase in surface area, resulting in an increased dissolution rate.

$$\frac{dC}{dt} = \frac{DS}{h} (C_s - C) \quad 2$$

Where dC/dt is dissolution rate, D is diffusion coefficient, S is the particle surface area, h is the thickness of the diffuse layer, C_s is the saturation solubility, C is the concentration of the drug in bulk solution. According to Equation (2), the dissolution rate of a drug into an aqueous solution depends on D , S , C_s , and h . Therefore, as particle size decreases, surface area increases, thereby leading to improved dissolution rates. In this study, the dissolution rate of nanosuspension, in comparison with the raw puerarin, was investigated.

Hence, for the nanosuspension, a much faster dissolution rate profile should have been observed. However, the dissolution results from the paddle apparatus (Figure 6B) illustrated the contrary, indicating much slower rates initially for the puerarin nanosuspension. This abnormality was attributed to the propensity of nanosuspension to form aggregates [10], leading to a reduced surface area and hence, slower dissolution rate. Visually, the nanosuspension was found floating on the surface of the dissolution medium, which was in good agreement to the findings of a researcher [23].

The dissolution profile for the basket apparatus (Figure 6A) showed that the nanosuspension began with smaller dissolution but gradually much faster than the raw puerarin. The basket method relied on forces outside of the basket to make the powder to the dissolution medium, but then the powder floated up to the surface of the dissolution medium, resulting in bad wetting. The most likely cause of this phenomenon was that the basket method did not generate adequate liquid flow past the surface of the powder particles, hence resulting in the eventual formation of aggregates inside the basket and the associated wetting problems. So, the results of basket method are not representative of the actual powder dissolution.

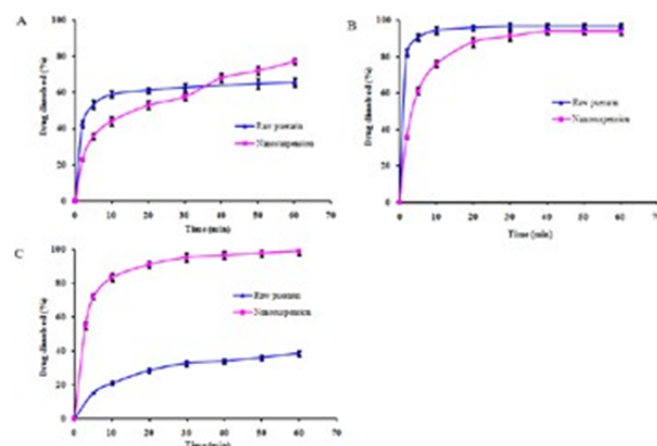


Figure 6: Dissolution profiles of raw puerarin and nanosuspension obtained from: A. basket apparatus, B. paddle apparatus, C. flow-through cell.

In the flow-through cell setup, the powder was held in place in the cell, hence minimizing any wetting or floating problems. Typical cumulative dissolution profiles were shown in Figure 6C. The dissolution rate was markedly enhanced in the nanosuspension, and nearly 100% of the drug dissolved within 60 min, as opposed to only 38.48% for the raw puerarin. This could be attributed to the increased surface area and enhanced saturation solubility of puerarin in the nanosuspension. The dissolution profiles showed excellent discriminatory behavior between the samples. These results thus provide direct evidence for the suitability of the flow-through cell for the analysis of nanoparticle dissolution.

In conclusion, the flow-through cell has been shown to be most suitable for dissolution analysis and performance evaluation of nanosuspension. According to a researcher, the ability of the flow-through method to discern the true extent of nanoparticle dissolution will be beneficial in the optimization of poorly soluble drugs and study of nanoparticle release rate [23].

4. CONCLUSIONS

An anti-solvent precipitation method was successfully employed to produce puerarin nanosuspension. The diameter of nanosuspension was about 195 nm (\pm 8 nm). Substantial crystalline change was found in nanosuspension compared with raw puerarin. The flow-through cell has been shown to be most suitable for dissolution analysis and performance evaluation of drug nanoparticles. Marked enhancement of dissolution rate was achieved by the reduction in particle size. The anti-solvent precipitation method is easy to apply and needs only simple equipment and, thus, is a promising method for preparing drug nanoparticles.

Further work on the oral bioavailability of the prepared puerarin nanosuspension is being carried out.

DECLARATION OF INTEREST

The authors report no declarations of interest.

ACKNOWLEDGMENTS

This work was financially supported by the National Nature Science Foundation of China (No. 81403111).

REFERENCES

- [1] Keck, C.M., Muller, R.H. 2006. Drug nanocrystals of poorly soluble drugs produced by high pressure homogenization, *European Journal of Pharmaceutics and Biopharmaceutics*, 62, 3-16.
- [2] Sigfridsson, K., Forssen, S., Hollander, P., Skantze, U., Verdier, J. 2007. A formulation comparison, using a solution and different nanosuspensions of a poorly soluble compound, *European Journal of Pharmaceutics and Biopharmaceutics*, 67, 540-547.
- [3] Gao, L., Zhang, D., Chen, M., Duan, C., Dai, W., Jia, L., Zhao, W. 2008. Studies on pharmacokinetics and tissue distribution of oridonin nanosuspensions, *International Journal of Pharmaceutics*, 355, 321-327.
- [4] Kassem, M.A., Abdel, R.A., Ghorab, M.M., Ahmed, M.B., Khalil, R.M. 2007. Nanosuspension as an ophthalmic delivery system for certain glucocorticoid drugs, *International Journal of Pharmaceutics*, 340, 126-133.
- [5] Jacobs, C., Muller, R.H. 2002. Production and Characterization of a Budesonide Nanosuspension for Pulmonary Administration, *Pharmaceutical Research*, 19, 189-194.
- [6] Shaal, L.A., Müller, R.H., Keck, C.M. 2010. Preserving hesperetin nanosuspensions for dermal application, *Pharmazie*, 65, 86-92.
- [7] Salazar, J., Ghanem, A., Muller, R.H., Moschwitz, J.P. 2012. Nanocrystals, comparison of the size reduction effectiveness of a novel combinative method with conventional top-down approaches, *European Journal of Pharmaceutics and Biopharmaceutics*, 81, 82-90.
- [8] Dong, Y., Ng, W.K., Shen, S., Kim, S., Tan, R.B. 2011. Controlled antisolvent precipitation of spironolactone nanoparticles by impingement mixing, *International Journal of Pharmaceutics*, 410, 175-179.
- [9] Chavhan, S.S., Petkar, K.C., Sawant, K.K. 2011. Nanosuspensions in drug delivery, recent advances, patent scenarios, and commercialization aspects, *Critical Reviews in Therapeutic Drug Carrier Systems*, 28, 447-488.
- [10] Horn, D., Rieger, J. 2001. Organic nanoparticles in the aqueous phase-theory, experiment, and use. *Angew, Angewandte Chemie International Edition*, 40, 4331-4361.
- [11] Guerra, M.C., Speroni, E., Broccoli, M., Cangini, M., Pasini, P., Minghetti, A. 2000. Comparison between chinese medical herb *Pueraria lobata* crude extract and its main isoflavone puerarin antioxidant properties and effects on rat liver CYP-catalysed drug metabolism, *Life Sciences*, 67, 2997-3006.
- [12] Liu, Q., Lu, Z., Wang, L. 2000. Restrictive effect of puerarin on myocardial infarct area in dogs and its possible mechanism, *Tongji Medical University*, 20, 43-45.
- [13] Lu, X.R., Gao, E., Xu, L.Z., Li, H.Z., Kang, B., Chen, W.N. 1987. Puerarin beta-adrenergic receptor blocking effect, *Chinese Medicine*, 100, 25-28.
- [14] Yue, P.F., Yuan, H.L., Zhu, W.F., Cong, L.B., Xie, H., Liu, Z.G. 2008. The study to reduce the hemolysis side effect of puerarin by a submicron emulsion delivery system, *Biological and Pharmaceutical Bulletin*, 31, 45-50.
- [15] Wang, Y., Ma, Y., Du, Y., Liu, Z., Zhang, D. 2012. Formulation and pharmacokinetics evaluation of puerarin nanocrystals for intravenous delivery, *Journal of Nanoscience and Nanotechnology*, 12, 6176-6184.
- [16] Dong, Y., Ng, W.K., Shen, S., Kim, S., Tan, R.B. 2009. Preparation and characterization of spironolactone nanocrystals by antisolvent precipitation, *International Journal of Pharmaceutics*, 375, 84-88.
- [17] Bhattachar, S.N., Wesley, A., Fioritto, J.A., Martin, P.J., Babu, S.R. 2002. Dissolution testing of a poorly soluble compound using the flow-through cell dissolution apparatus, *International Journal of Pharmaceutics*, 236, 135-143.
- [18] Wong, J., Brugger, A., Khare, A., Chaubal, M., Papadopoulos, P., Rabinow, B. 2008. Suspensions for intravenous (IV) injection, a review of development, preclinical and clinical aspects, *Advanced Drug Delivery Reviews*, 60, 939-954.
- [19] Sahoo, N.G., Abbas, A., Judeh, Z., Li, C.M., Yuen, K.H. 2009. Solubility enhancement of a poorly water-soluble anti-malarial drug: experimental design and use of a modified multifluid nozzle pilot spray drier, *Journal of Pharmaceutical Sciences*, 98, 281-296.
- [20] Douroumis, D., Fahr, A. 2007. Stable carbamazepine colloidal systems using the cosolvent technique, *European Journal of Pharmaceutical Sciences*, 30, 367-374.
- [21] Raghavan, S.L., Trividic, A., Davis, A.F., Hadgraft, J. 2001. Crystallization of hydrocortisone acetate, influence of polymers, *International Journal of Pharmaceutics*, 212, 213-221.
- [22] Muller, R.H., Peters, K. 1998. Nanosuspension for formulation of poorly soluble drugs I: preparation by size reduction technique, *International Journal of Pharmaceutics*, 160, 229-237.
- [23] Heng, D., Cutler, D.J., Chan, H.K., Yun, J., Raper, J.A. 2008. What is a suitable dissolution method for drug nanocrystals, *Pharmaceutical Research*, 25, 1696-1701.

